Biogeosciences Discuss., doi:10.5194/bg-2015-533, 2016
Manuscript under review for journal Biogeosciences
Published: 22 February 2016

Biogeosciences Discussions
Open Access
EGU

Rates and pathways of CH_4 oxidation in ferruginous Lake Matano, Indonesia

A. Sturm[1], D. A. Fowle[1], C. Jones[2,4], K. Leslie[1], S. Nomosatryo[3], C. Henny[3], D. E. Canfield[4], and S. A. Crowe[2,4]

[1]Department of Geology, University of Kansas, Lawrence KS 66047, USA
[2]Department of Microbiology and Immunology and Department of Earth, Ocean, and Atmospheric Sciences, University of British Columbia, 2350 Health Sciences Mall, Vancouver, British Columbia V6T 1Z3, Canada
[3]Research Center for Limnology, Indonesian Institute of Sciences (LIPI), Cibinong-Bogor, Indonesia
[4]Nordic Center for Earth Evolution, Institute of Biology, Univ. of Southern Denmark, Campusvej 55, 5230 Odense, Denmark

Received: 14 October 2015 – Accepted: 15 October 2015 – Published: 22 February 2016

Correspondence to: S. A. Crowe (sean.crowe@ubc.ca)

Published by Copernicus Publications on behalf of the European Geosciences Union.

Abstract

This study evaluates rates and pathways of methane (CH_4) oxidation and uptake using ^{14}C-based tracer experiments throughout the oxic and anoxic waters of ferruginous Lake Matano. Methane oxidation rates in Lake Matano are low compared to other lakes, but are sufficiently high to preclude strong CH_4 fluxes to the atmosphere. In addition to aerobic CH_4 oxidation, which takes place in Lake Matano's oxic mixolimnion, we also detected CH_4 oxidation in Lake Matano's anoxic ferruginous waters. Here, CH_4 oxidation proceeds in the apparent absence of oxygen (O_2) and instead appears to be coupled to nitrate (NO_3^-), nitrite (NO_2^-), iron (Fe), or manganese (Mn) reduction. Throughout the lake, the fraction of CH_4 carbon that is assimilated vs. oxidized to carbon dioxide (CO_2) is high, indicating extensive CH_4 conversion to biomass and underscoring the importance of CH_4 as a carbon and energy source in Lake Matano and potentially other ferruginous or low productivity environments.

1 Introduction

Methane (CH_4) is a critical component of the global carbon cycle and is a potent greenhouse gas (Cicerone and Oremland, 1988; Conrad, 2009; Kroeger et al., 2011). Indeed, dramatic changes in global climate throughout Earth's history have been linked to alterations in the global CH_4 cycle (Kroeger et al., 2011; Sloan et al., 1992; Zeebe et al., 2009). Methane is produced in the environment as the end product of organic matter degradation via methanogenesis, either through acetate fermentation or CO_2 reduction in freshwater and marine sediments and soils. A significant fraction of this CH_4 is then consumed through microbially catalyzed oxidation directly within soils and sediments or within water columns. Microbial oxidation of CH_4 can take place aerobically, with O_2 as the electron acceptor, or anaerobically (AOM), typically with sulfate (SO_4^{2-}) as the electron acceptor (Boetius et al., 2000; Devol et al., 1984; Martens and Berner, 1974; Reeburgh, 1980). Indeed, sulfate-dependent anaerobic CH_4 oxidation

BGD
doi:10.5194/bg-2015-533

consumes most of the CH_4 produced in marine sediments (Devol et al., 1984; Knittel and Boetius, 2009; Martens and Berner, 1974; Reeburgh, 2007; Treude et al., 2005) and is therefore the largest natural sink for CH_4 on the planet (Reeburgh, 2007). The scarcity of SO_4^{2-} in freshwater settings, however, is thought to largely preclude AOM, thus aerobic CH_4 oxidation is believed to dominate CH_4 consumption in these environments.

Large uncertainties accompany CH_4 budgets for freshwater environments due to physical and chemical diversity of lake, wetland, and soil systems, (Liikanen and Martikainen, 2003; Liikanen et al., 2003; Luesken et al., 2011a). Large intervals of diffusion limited marine sediments contain abundant sulfate and are therefore favorable to AOM. These represent a more effective CH_4 sink than the often narrow layers of oxic marine sediment that typically support aerobic methanotrophy. Sulfate concentrations are generally much lower in freshwater systems and, without expansive zones supporting sulfate-dependent AOM, may not be as effective at total CH4 removal as their marine counterparts. Thus, freshwater systems emit proportionally much more CH_4 to the atmosphere (Capone and Kiene, 1988; Conrad, 2009).

Recently, evidence has emerged for AOM utilizing alternative electron acceptors. Nitrate dependent AOM takes place in enrichment cultures from NO_3^- and NO_2^- rich canal waters (Raghoebarsing et al., 2006) and wastewater systems (Kampman et al., 2012; Luesken et al., 2011a, b; Shen and Hu, 2012). Isolates of *Methylomirabilis oxyfera* conduct nitrate-dependent CH_4 oxidation through a novel denitrifying pathway (Ettwig et al., 2010). Other NO_3^--dependent CH_4 oxidizing archaea couple NO_3^- reduction to ammonium (NH_4^+) with CH_4 oxidation (Haroon et al., 2013). Despite abundant documentation of NO_3^- dependent AOM in lab settings and wastewaters, its broader significance in natural environments is largely unknown at this time. However, natural systems rich in NO_3^- with rapid N-cycling, such as freshwater lakes, estuaries, and wetlands, should have the potential to oxidize immense amounts of CH_4 through NO_3^- dependent AOM (Joye et al., 1999). Evidence for Fe and Mn dependent CH_4 oxidation is also accruing and has been proposed to explain geochemical evidence for AOM in

BGD
doi:10.5194/bg-2015-533

freshwater environments in the apparent absence of SO_4^{2-} (Crowe et al., 2008a, 2011; Lopes et al., 2011; Nordi et al., 2013; Sivan et al., 2011). However, these environmental observations remain unsubstantiated, and AOM in these systems has not been confirmed by process rate measurements or shown through microbial isolation and pure culture laboratory experiments.

Lake Matano, Sulawesi Island, Indonesia, hosts the largest, deepest, and oldest known ferruginous basin on Earth (Crowe et al., 2008a, b). This system offers a unique opportunity to examine CH_4 biogeochemistry under conditions with very low natural SO_4^{2-} concentrations and an abundant supply of Fe and Mn oxyhydroxides. In general, tropical lakes are understudied by comparison to their temperate counterparts. Further examination of such systems is needed to constrain global CH_4 budgets. Furthermore, with chemistry and physics analogous to those proposed for the Precambrian oceans, Lake Matano also affords opportunities to test models for the marine CH_4 cycle throughout much of Earth's history. To betterconstrain CH_4 biogeochemistry in Lake Matano, tropical lakes, and ferruginous environments in general, we have determined CH_4 oxidation rates with a suite of oxic and anoxic incubations using ^{14}C labeled CH_4. These rate measurements are interpreted with respect to the availability of oxidants to place constraints on the pathways of CH_4 oxidation throughout the lake.

2 Materials and methods

2.1 Sampling and general analyses

Samples were retrieved from a deep-water master station (2°28′00″ S and 121°17′00″ E) (Crowe et al., 2008b) in May 2010. For deep and shallow water sampling (i.e. < 100 m or > 140 m) 5 L Go-Flow (Niskin; General Oceanics, Miami, FL, USA) bottles were used with a manual winch setup and a Furuno FCV585 sonar device for bottle placement by echolocation, achieving an accuracy and precision of ±1 m. For samples in intermediate depths (i.e. > 100 m, < 140 m deep), a pump profiling method was used

BGD
doi:10.5194/bg-2015-533

(Jones et al., 2011) in which water was pumped from depth using a double-cone intake (Jørgensen et al., 1979) sampling a thin (< 2 cm) horizontal layer of water. The intake was fastened to a conductivity, temperature, depth (CTD) probe (Sea and Sun Technology), which allowed for very accurate (~ 10 cm) vertical sample positioning during pumping. A minimum of three tubing volumes of water was flushed through the tubing and pump system before sampling commenced. Oxygen concentrations, conductivity and temperature were determined using the CTD equipped with the following sensor array: temperature (SST PT100, accuracy ± 0.005 °C, precision ± 0.001 °C), conductivity (SST 7-pole platinum cell, accuracy ± 0.005 mS cm^{-1}, precision±0.0001 mS cm^{-1}), O_2 (Oxyguard Ocean (2009), Oxyguard Profile (2010), detection limit ~ 1 % saturation, precision ± 1 % saturation), light (LICOR PAR Sensor 193 SA, Accuracy ± 5 %, detection limit 0.01 µmol m^{-2} s^{-1}), and turbidity (Seapoint). In addition to the measurements made using the Oxyguard sensors on the CTD, O_2 concentrations were also determined using the classic Winkler titration (detection limit 6 µmol L^{-1}) (APHA, 1985; Rose and Long, 1988). The position of the oxycline was verified independently in pumped water with surface based measurements using potentiometry with Clark-style microelectrodes (Unisense) (detection limit 0.2 µmol L^{-1}), and by voltammetry using Au/Hg amalgam microelectrodes (1 µmol L^{-1}) (Brendel and Luther, 1995) (data not shown). Samples for measurement of Fe^{2+} concentrations were withdrawn directly from the pump stream or the spout of the Niskin bottle and fixed on site with ferrozine reagent, stored refrigerated (4 °C), and analyzed by a standard spectrophotometric method (Stookey, 1970; Viollier et al., 2000) within 8 h. Nitrite and NO_3^- combined NO_x, was determined by chemiluminescnce (Braman and Hendrix, 1989) and SO_4^{2-} by ion chromatography (Dionex ICS 1500, with an IONpac AS22 anion column and suppressor). Samples for CH_4 concentrations were withdrawn directly from the Niskin bottle spout or pump tubing via a syringe and needle and introduced directly into pre-evacuated serum bottles with thick, butyl rubber stoppers, which were poisoned immediately with 100 µL of concentrated $HgCl_2$ (Crowe et al., 2011) to prevent methanogenesis or CH_4 oxidation. Methane concentrations were measured by gas chromatography (Agilent

BGD
doi:10.5194/bg-2015-533

Technologies Network GC System 6890N), and depending on concentration, using either Thermal Conductivity Detection (TCD) or Flame Ionization Detection (FID).

2.2 Incubations

2.2.1 General incubation setup

Water for incubations was sampled from the lake as described above and transferred directly into 100 mL glass syringes (110, 115, 120, and 130 m) or 60 mL plastic syringes (20, 39.5, 81.7, and 105.2 m). Here, it is important to note that the glass syringes were used for the sample depths that were evidently anoxic or in the oxic–anoxic transition zone such as the 110 m depth sample. The plastic syringes were used only for oxic depth intervals. All syringes were flushed with three volumes of water from the depth of interest and were filled without gas headspace. The openings of the syringes were closed with long (1.5″) 25 gauge needles, which were plugged with high-density butyl rubber stoppers. The O_2 concentration was measured inside the syringes immediately following sampling with a standard Clark-style O_2 electrode, inserting it into the luer-lock opening of the syringe. Oxygen was below detection (250 nmol L^{-1}) in the syringes from depths 110 m through to 130 m.

Radiolabeled CH_4 dissolved in water (2.3–4.5 *n*Ci/incubation, 5–10 µL of 10 µmol L^{-1} CH_4 at an activity of 45.04 Ci mol^{-1}) was injected into the syringes by inserting a long needle into the luer-lock tip of the syringe in order to prevent the introduction of atmosphere. The syringes were closed immediately after the label addition, and a small amount of water was expelled to insure that there were no air bubbles trapped in the needle closure. The syringes were then incubated under water in the dark at an ambient temperature of ~ 28 °C for 6 to 18 days, with sampling intervals extending from between 30 min and several hours initially to several days at the end.

Incubation sampling was conducted by removing the rubber stopper on the end of the syringe needle, flushing a small amount of water out of the needle, and then inserting the needle into an evacuated 12.5 mL Exetainer containing 1 mL of 4 M NaOH.

BGD
doi:10.5194/bg-2015-533

Once the Exetainer pressure was at equilibrium with the syringe (~ 1 atm), the needle was removed, plugged with the butyl rubber stopper, and the syringe immediately returned to the water bath. At the end of the incubation period, the O_2 concentration was again measured inside the syringe with a Clark-style O_2 electrode. Oxygen was below detection (250 nmol L^{-1}) in the syringes sampled from 110 m through to 130 m. Exetainers were stored upside down and refrigerated at 4 °C except during air transport from Indonesia to Denmark.

2.2.2 Oxygen introduction to glass syringes

To estimate the possible introduction of O_2 into the glass syringes by diffusion along the ground glass syringe piston over the incubation period, we computed the O_2 fluxes along the syringe walls. Fluxes were calculated according to Fick's first law:

$$J = D\frac{\partial O_2}{\partial x} \quad (1)$$

where J is the O_2 flux, D is the calculated O_2 diffusivity (2.55386×10^{-5} cm^2 s^{-1}) (Wilke and Chang, 1955; Reid et al., 1977), $\partial[O_2]$ is the difference in O_2 concentration between the outside and inside of the syringe, and ∂x the distance along the piston from the outside of the syringe to the water inside. The piston glass is ground along the whole length of insertion, increasing the diffusion path length ∂x every time the piston was pushed further into the syringe when extracting sample (Table S1 in the Supplement). The value for $\partial[O_2]$ was set as a constant, assuming water in the syringes was anaerobic and water outside of the syringes was at saturation with respect to the atmosphere (250 µmol L^{-1}). The variable ∂x depended on the volume remaining in the syringe and ranged from 55 to 153 mm, at 100 and 0 mL syringe volume, respectively. The total O_2 flux into the syringes was calculated by the product of J and the area estimated between the piston wall and the inside of the syringe. Since tolerances for our syringes were not obtainable, this area was conservatively estimated by multiplying the available tolerances (0.0065 mm, Northern Technology and Testing®:

BGD
doi:10.5194/bg-2015-533

http://www.nttworldwide.com/docs/specs100ml.pdf) for glass syringes by 30 to yield an area of 21.5 mm^2. Summaries of possible O_2 introduction rates are given in Tables S1, S2 and Figs. S1, S2 in the Supplement. Introduction of O_2 into the glass syringes could have occurred at a maximum flux of 11.6 $nmol\,m^{-2}\,s^{-1}$, with the potential to oxidize CH_4 at a maximum rate of 215 $nmol\,L^{-1}\,d^{-1}$.

2.2.3 Oxygen introduction to plastic syringes

To estimate the possible O_2 introduction into the plastic syringes over the incubation period, we computed the O_2 fluxes through the plastic syringe walls. These fluxes were also calculated using Fick's first law with O_2 diffusivity through the polyethylene syringes of $D = 4.60 \times 10^{-8}\,cm^{-2}\,s^{-1}$ (Trefry and Patterson, 2001). Different initial O_2 concentrations produce different O_2 gradients for each sample depth, which translate to different diffusion rates. The value for $\partial[O_2]$ was set as a constant with the outside of the syringe at saturation with respect to the atmosphere (250 $\mu mol\,L^{-1}$), and the inside of the syringe set at the measured water column $[O_2]$ for the relevant depth intervals. The O_2 concentrations were expected to remain the same over the duration of the CH_4 oxidation rate measurements owing to low total respiration rates in Lake Matano (SA Crowe, unpublished data). Diffusion path length ∂x was set to 0.1 cm, the wall thickness of the syringe. The total flux into the syringe was calculated by multiplying F by the area of the syringe, which varied linearly from 99.66 to 29 cm^2, with a full 60 and 10 mL of water in the syringe, respectively. Summaries of O_2 introduction into the plastic syringes are provided in the Supplement and ranged from 0.97 $\mu mol\,d^{-1}$ (105 m, T_o) to 0.11 $\mu mol\,d^{-1}$ (20 m, T_F).

2.2.4 Measurement of radioactivity

Samples for the oxidation rate measurements were processed according to previously established methods (Iversen and Blackburn, 1981). Methane was flushed out of the Exetainer for 30 min at a flow-rate of 17 $mL\,min^{-1}$ via two needles, one needle sup-

BGD
doi:10.5194/bg-2015-533

plying a CH_4 and air carrier gas mix (2 % CH_4) into the Exetainer and the other leading to a copper catalyst housed in a tube furnace, where the CH_4 was oxidized at 850 °C. The CO_2 produced was trapped directly in 20 mL scintillation vials filled with 2-phenylethylamine (4 mL) and methanol (4 mL), which has the capacity to capture 2 orders of magnitude more CO_2 than was produced by the CH_4 combustion. Immediately following CO_2 capture, 10 mL of scintillation cocktail (Ultima Gold XR, Packard) was added to the vials, which were vortexed for 1 min. The samples were then left to stand for 24 h before they were counted on the scintillation counter (Perkin-Elmer-Tri-Carb 2910 TR). Methane oxidation efficiency tests were performed and resulted in a CH_4 to CO_2 conversion greater than 99.8 % at carrier-gas CH_4 concentrations of 2 %.

To extract the CO_2 from the remaining liquid in the Exetainer, 1–2 drops of bromothymol blue was added to the sample to monitor sample pH and the sample was placed into an Erlenmeyer flask along with a 20 mL scintillation vial containing a folded fiberglass filter wet with 4 mL of 2-phenylethylamine. The Erlenmeyer flask was sealed with a thick, butyl rubber stopper through which a long needle was inserted to inject 2 mL of hydrochloric acid (6 M) into the Exetainer to exsolve the CO_2. The pH was checked visually after 24 h, and the samples were left for a total of 48 h to allow the complete exsolution of CO_2 and its effective entrapment on the phenylethylamine soaked filter. The scintillation vials were removed from the Erlenmeyer flasks, and 4 mL of methanol was added to dissolve the precipitate, after which 10 mL of scintillation cocktail was added and the entire contents vortexed for 2 min. These samples were then left to stand for 24 h before scintillation counting. To measure the assimilation of ^{14}C carbon from CH_4 during the incubations, 3 mL of the residual fluid from each Exetainer vial was transferred into a scintillation vial and 10 mL of Scintillation cocktail added. The sample was vortexed for 1 min, after which it stood for 24 h before counting. Methane oxidation and assimilation were determined from concentrations and activities using Eqs. (2) and (3). Methane oxidation and assimilation rates were then computed as first order rates from

BGD
doi:10.5194/bg-2015-533

the linear portion of the time series with two or more intervals.

$$[CH_{4oxidized}] = [CH_4]^{14}CO_2/^{14}CH_4 \quad (2)$$

$$[CH_{4assimilated}] = [CH_4]^{14}C_{residual}/^{14}CH_4 \quad (3)$$

All data used in rate calculations are tabulated in the (Table S3 in the Supplement).

3 Results

3.1 Limnology

The physical structure of Lake Matano in 2010 was much the same as previously observed (Figs. 1 and 2). During our sampling expedition, the lake was stratified with a persistent pycnocline between 110 and 250 m depth, which separates an oxic mixolimnion from a permanently anoxic monimolimnion. The mixolimnion exhibits a previously observed seasonal pycnocline (Crowe et al., 2011), which at the time of our sampling was at a depth of 30 m. A slow exchange of water across the persistent pycnocline at 110 m depth produces poorly ventilated bottom waters, which was indicated by the exhaustion of O_2 and the accumulation of Fe^{2+}. Reduced iron increases to detectable concentrations (0.2 µmol L^{-1}) just below the depth at which O_2 becomes undetectable (1 µmol L^{-1}) at 112–114 m depth (Fig. 3). Due to the rapid oxidation kinetics of Fe^{2+} by O_2, it was unlikely that appreciable concentrations of O_2 coexisted with detectable Fe^{2+}, and we thus define the oxic–anoxic boundary as the layer between the deepest depth of detectable O_2 and the shallowest depth at which Fe^{2+} is detected.

Most of the redox active species (Fe^{2+}, Mn^{2+}, SO_4^{2-}, HS^-) followed the classical redox cascade (Canfield and Thamdrup, 2009; Jones et al., 2011): O_2 and Mn^{2+} overlaped slightly (Fig. 3a), which can be explained by the sluggish oxidation kinetics of Mn^{2+} with O_2 (Jones et al., 2011; Luther, 2005; Morgan, 2005). Nitrite and NO_3^- (NO_x) accumulated in the lower mixolimnion (Fig. 3b), with a maximum concentration

BGD
doi:10.5194/bg-2015-533

of 6 µmol L^{-1} at 111 m. Fe and Mn particulates (Fig. 3c) also exhibited peaks in concentration near the pycnocline (Jones et al., 2011). Fe^{2+} and NH_4^+ (Fig. 3a) were both below detection in the surface waters with a sharp increase at the oxic–anoxic boundary and had constant deep-water concentrations below approximately 250 m depth.

3.2 Oxic water column

Methane concentrations in the oxic water column were 0.5 µmol L^{-1} and were oversaturated with respect to the atmosphere. Methane consumption during the 20, 39.5, and 81.7 m incubations was negligible (0.53, 0.65, and 0.13 %) for the time interval in which the rates were measured (Table 2). Rates of dissimilatory CH_4 oxidation (CH_4 oxidation), where CH_4 is converted into CO_2, between 20 and 39.5 m range from (0.2 to 0.43 nmol L^{-1} d^{-1}) in the fully oxygenated mixolimnion (Fig. 4) and remained almost the same at 81.7 m with 0.37 nmol L^{-1} d^{-1}. Rates of CH_4 assimilation into organic matter (CH_4 assimilation) ranged from 0.13 to 2.43 nmol L^{-1} d^{-1} in the mixolimnion, and summing the rates of CH_4 assimilation with the rates of dissimilatory CH_4 oxidation yielded total CH_4 consumption rates (total consumption) of 0.36 to 2.51 nmol L^{-1} d^{-1}. Oxygen concentrations in the upper water column were near saturation with respect to the atmosphere and were above 200 µmol L^{-1}, though O_2 became depleted with increasing depth and concentrations were 138 µmol L^{-1} at 39.5 m and 58.4 µmol L^{-1} at 81.5 m (Table 2).

3.3 Oxic–anoxic transition layer

Rates of CH_4 oxidation within this layer were between 78 nmol L^{-1} d^{-1} at 105 m depth and 527 nmol L^{-1} d^{-1} at 110 m depth; rates of CH_4 assimilation ranged from 142 to 3640 nmol L^{-1} d^{-1} (105–110 m). Summing the rates of CH_4 assimilation and dissimilatory CH_4 oxidation yielded total CH_4 consumption in the oxic–anoxic transition layer that ranged from 220 to 4160 nmol L^{-1} d^{-1} (Fig. 4). Average O_2 concentrations

BGD
doi:10.5194/bg-2015-533

within this layer were less than 3 µmol L^{-1}, whereas CH_4 concentrations ranged from 6.98 µmol L^{-1} at 105 m to 2.70 µmol L^{-1} at 110 m.

3.4 Upper anoxic zone

With 2.6 µmol L^{-1} of Fe^{2+} at 115 m, the upper monimolimnion is strictly anoxic. Rates of CH_4 oxidation in this layer ranged from 5.6 µmol L^{-1} d^{-1} at 115 m depth to 50.1 µmol L^{-1} d^{-1} at 130 m depth. Rates of CH_4 assimilation were 6.3 µmol L^{-1} d^{-1} at 115 m and 67.2 µmol L^{-1} d^{-1} at 130 m. Total CH_4 consumption at these depths was 11.9 µmol L^{-1} d^{-1} at 115 m and 117.4 µmol L^{-1} d^{-1} at 130 m. Methane concentrations over the 115 to 130 m depth interval ranged from 12 to 484 µmol L^{-1}, $^{\cdot}NO_x$ concentrations were 0.06 to 0.5 µmol L^{-1}, and Fe and Mn oxyhydroxide concentrations were 95–170 nmol L^{-1} and 1–361 nmol L^{-1}, respectively. Sulfate concentrations ranged from 0.6 to 19.6 µmol L^{-1}, and SO_4^{2-} reduction rates were on the order of 0.93–4.73 nmol L^{-1} d^{-1} over the 115 to 130 m depth interval.

4 Discussion

4.1 Oxidation in the oxic water column

Methane oxidation rates from a variety of well-oxygenated environments (> 25 µmol L^{-1}) have been compiled (Table 1) to provide a comparison to the rates measured in Lake Matano. The upper mixolimnion maintained CH_4 oxidation rates in the lower range compared to other aquatic environments (Table 1). The kinetics of aerobic microbial CH_4 oxidation are typically described by a Michaelis–Menten model with half-saturation constants for CH_4 typically between 2 and 26 µmol L^{-1} (Buchholz et al., 1995; Harrits and Hanson, 1980; Lidstrom and Somers, 1984; Remsen et al., 1989) and for O_2 0.14 to 21 µmol L^{-1} (Joergensen, 1985; Lidstrom and Somers, 1984). With CH_4 concentrations below K_m values, CH_4 oxidation rates in the mixolimnion were likely lim-

BGD
doi:10.5194/bg-2015-533

ited by CH_4 availability. Though CH_4 concentrations in Lake Matano's mixolimnion were low, ranging from 0.5 to 3 µmol L^{-1}, and below typical K_m values for methanotrophs, they are still well above threshold in vitro concentrations (50 to 150 nmol L^{-1})(Schmidt and Conrad, 1993; Whalen et al., 1990), below which CH_4 oxidizing microbes can no longer access dissolved CH_4. High O_2 concentrations (> 120 µmol L^{-1}, or > 48 % of saturation) are also known to inhibit CH_4 oxidation (Harrits and Hanson, 1980) and thus at 20 m depth, CH_4 oxidation may have also been inhibited by as much as 58 % due to high O_2 concentration. However, below 45 m (< 120 µmol L^{-1} O_2) inhibition due to O_2 would be unlikely (Harrits and Hanson, 1980).

4.2 Oxidation in the oxic–anoxic transition layer

Rates for CH_4 oxidation at 105 and 110 m (Fig. 4), in the oxic–anoxic transition layer, were higher than in the oxic zone. These rates were within the range reported for comparable freshwater systems (Table 1). In all systems in Table 1, O_2 concentrations were reported between 2.5–25 µmol L^{-1}, and CH_4 concentrations were in the low µmol L^{-1} range. Lake Matano's rates of CH_4 oxidation in the oxic–anoxic transition layer averaged 219 nmol L^{-1} d^{-1}. This is in the low to mid portion of the range observed in other freshwater bodies, which varies 9 orders of magnitude (Table 1). Since both O_2 and CH_4 concentrations were low within the oxic–anoxic transition zone, the rates were likely dictated by the co-availability of O_2 and CH_4. This is supported by laboratory-based studies of CH_4 oxidation kinetics (Buchholz et al., 1995; Harrison, 1973; Joergensen, 1985; Lidstrom and Somers, 1984).

Given the low O_2 concentrations in this depth interval we sought to constrain the possible availability of alternative electron acceptors for CH_4 oxidation through a mass balance approach. Based on mass balance considerations, the O_2 present at 105 m was sufficient to support the measured rates. At 110 m depth, O_2 was below the detection limit (0.25 µmol L^{-1}) of our O_2 sensor. Over the time interval of the rate determination, 0.114 µmol L^{-1} O_2 would have been sufficient to oxidize the CH_4 con-

BGD
doi:10.5194/bg-2015-533

sumed, and therefore if 0.25 µmol L^{-1} O_2 was present, yet under the detection limit of our microsensor measurements, this would provide sufficient O_2 (Table 2). Our calculations also suggest rates of O_2 diffusion into the syringe of between 1.16×10^{-6} and 4.21×10^{-7} µmol cm^{-2} s^{-1}, could have supplied up to 19 % of the total O_2 needed to match the observed CH_4 oxidation. We argue, then, that no alternative electron acceptors were needed to support the observed rates of CH_4 oxidation in the oxic–anoxic transition layer. Nevertheless, total CH_4 consumption at the 110 m depth was 0.448 µmol L^{-1}, with 0.391 µmol L^{-1} attributed to assimilation. If, however, assimilated CH_4 was also oxidized during the assimilation process, the O_2 available would not be sufficient to oxidize this CH_4, and other electron acceptors would need to be considered. Measurements for particulate Fe and Mn were not taken at this depth, but if concentrations are similar to samples below and above this depth, combined concentrations should have been between 30 and 300 nmol L^{-1} and can therefore only account for a fraction of the oxidation needed. Sulfate and NO_x were both present in quantities that would satisfy the demand for electron acceptors, but SO_4^{2-} reduction rates of only a few nmol L^{-1} d^{-1} rule out its involvement in CH_4 oxidation of this magnitude, leaving NO_x as the likely electron acceptor at the depth of 110 m.

4.3 Oxidation in the anoxic waters

Methane oxidation was also observed in incubations of water from depths (115, 120, and 130 m) below the oxic–anoxic transition zone (Fig. 4). This observation requires us to carefully consider the possible oxidants available. As above, we first consider possible O_2 contamination by diffusion into the syringes, which ranged from 1.16×10^{-6} to 7.28×10^{-7} µmol O_2 cm^{-2} s^{-1} (Table S1 in the Supplement) and can contribute at most 1.86, 11.8, and 0.216 % at 115, 120, and 130 m, respectively to the observed CH_4 oxidization (Table 2). There are several other theoretically possible oxidants (SO_4^{2-}, NO_2^-, NO_3^-, Fe^{3+}, Mn^{4+}) for which reactions are given in Table 3.

BGD
doi:10.5194/bg-2015-533

To validate if these electron acceptors are suitable, we have calculated $\Delta_r G$ values for each electron acceptor considering the in situ conditions in Lake Matano. The possible Gibbs free energy space defined by substrate concentrations in Lake Matano is marked in green on the graphs in Fig. 5 along with energies calculated specifically for the three anoxic samples at 115, 120, and 130 m depth. The conditions at which the ΔG's are −30 and −15 kJ mol^{-1} (Iso-energies) are marked in blue and red, identifying the lowest energies necessary for the generation of ATP and energies observed in similar environments known to support microbial growth, respectively (Caldwell et al., 2008; Hoehler et al., 1994; Valentine and Reeburgh, 2000). These boundaries, hence, are the lowest known amounts of energy at which organisms can grow using these metabolic pathways. All electron acceptors considered provide more than this minimum amount of free energy, except for SO_4^{2-}, which is close to the minimum energies (Fig. 5).

Concentrations of electron acceptors and their possible contribution to CH_4 oxidation in %, based on the reactions listed in Table 3, are given in Table 2 for each depth. Nitrite and NO_3^- are combined as NO_x, and Fe^{3+} and Mn^{4+} are referred to as Mn_{part} and Fe_{part}, since they primarily exist as particles in these oxidation states. The concentrations of available reactive Fe^{3+} and Mn^{3+}/Mn^{4+} were low, approximately 250–530 nmol s L^{-1} cumulative between 115 and 120 m and less than 100 nmol s L^{-1} at 130 m, compared to the amount of CH_4 oxidation observed, and could only account for up to 7.7, 22.1, and 0.37 %, respectively, of the CH_4 oxidation measured (Table 2). Nitrate-nitrite contributions to the oxidation of CH_4 would be low at 115 m and considerable at 120 m with 7.6 and 64 %, and then sink to a negligible 0.8 % at the 130 m depth. The only other significant oxidant at 115 and 120 m was SO_4^{2-}, which could account for all the CH_4 oxidation observed at these depths, though at 130 m, SO_4^{2-} was below our detection (> 250 nmol L^{-1}), a concentration at which SO_4^{2-} could only contribute 7.5 % to the CH_4 oxidation observed (Table 2). Similar to the oxic–anoxic transition layer, despite the apparent availability of SO_4^{2-} as an electron acceptor, the measured SO_4^{2-} reduction rates at these depths were less than 5 nmol L^{-1} d^{-1} (Fig. 4c). This suggests

BGD
doi:10.5194/bg-2015-533

that CH_4 oxidation coupled to SO_4^{2-} reduction alone cannot support the observed rates of AOM between the depths of 115 to 130 m. We are thus left with some uncertainty as to specific electron acceptors involved in CH_4 oxidation at Lake Matano given our inability to constrain the electron mass balance. It is likely, however, that we have underestimated the concentrations of particulate Fe and Mn (Jones et al., 2011). Particles too small to be retained on 0.2 µm filters, for example, may have escaped measurement. Such small particles have been observed in the lake as nano-particulate aggregates containing Fe and Mn using SEM and TEM (Jones et al., 2011; Zegeye et al., 2012) and would be among the most reactive of all the particles in the system. Though O_2 concentrations were measured in the syringes and all were below our DL (250 nmol L^{-1}), O_2 contamination could have occurred during sample handling but evaded detection due to its consumption by Fe^{2+} prior to measurement. For example, if sampling introduced 1–2 µmol L^{-1} O_2 this could have been rapidly consumed through oxidation of Fe^{2+}, supplying 4 to 8 µmol L^{-1} additional reactive Fe oxyhydroxides. Regardless of the uncertainties in available electron acceptors, the potential rates of anaerobic CH_4 oxidation measured are high, even in comparison to rates measured in other fresh (Iversen et al., 1987; Joye et al., 1999) and marine water columns (Wankel et al., 2010).

4.4 CH_4 assimilation

In Lake Matano a large fraction of CH_4 metabolized (up to 87 %) was assimilated (Fig. 6). The fraction of CH_4 carbon assimilated in Lake Matano is indeed as high as values reported in early isolation and characterization laboratory studies (80 % and 47–70 %) (Brown et al., 1964; Vary and Johnson, 1967). Most studies of temperate lakes report that about one-third of the carbon from CH_4 consumption was assimilated with two-thirds oxidized to CO_2 (Hanson, 1980; Harrits and Hanson, 1980; Lidstrom and Somers, 1984; Rudd et al., 1974). For example, the temperate meromictic Lake 120 of the Experimental Lake Area of Northern Ontario (Rudd et al., 1974), which, like Lake Matano, is persistently stratified, exhibited only 36.8 % assimilation. Perhaps because

BGD
doi:10.5194/bg-2015-533

of its physical and chemical similarities, the most appropriate comparison is Lake Tanganyika, which exhibits on average 26 % assimilation (Rudd, 1980). We suggest that the high percentage of assimilation in Lake Matano may reflect its highly oligotrophic nature. In more productive systems, excess organic carbon is available for growth, thus most CH_4 carbon is channeled through dissimilation to CO_2 (Rudd, 1980). Anecdotally, carbon assimilation from CH_4 in marine systems is generally higher than in freshwater systems (Ward et al., 1987) and marine systems are typically more oligotrophic than freshwater.

These relative high rates of CH_4 assimilation suggest that CH_4 may be an important source of carbon for biomass in Lake Matano. Though rates of CH_4 assimilation within the surface waters (10 m, 0.2 nmol L^{-1} d^{-1}) are small compared to dark carbon fixation rates (14 nmol L^{-1} d^{-1}), the deeper anoxic waters exhibit CH_4 assimilation rates of up to 8.2 µmol L^{-1} d^{-1} (120 m) which exceeds dark carbon fixation rates of 0.24 µmol L^{-1} d^{-1} (at 117.5 m) by 34 times, implicating CH_4 assimilation as the largest carbon fixing process within this depth interval.

5 Conclusions

Despite the accumulation of CH_4 to relatively high concentrations in Lake Matano's deep monimolimnion, much of this CH_4 is oxidized directly within the lake, precluding strong CH_4 fluxes to the atmosphere. Lake Matano, indeed, supports relatively high rates of CH_4 oxidation with some CH_4 apparently oxidized anaerobically (for example, rates of oxidation up to 5.6 µmol CH_4 L^{-1} d^{-1} occur at 115 m depth in the apparent absence of O_2). Alternative electron acceptors that may support measured AOM include NO_x, the oxidized forms of Fe and Mn, and SO_4^{2-}. Measured rates of SO_4^{2-} reduction are, however, too low to support the measured rate of CH_4 oxidation, and we favor NO_x and oxidized Fe and Mn as the likely electron acceptors. Lake Matano also exhibits unusually high rates of CH_4 assimilation, which may be related to its oligotrophic

BGD
doi:10.5194/bg-2015-533

nature. Regardless, such high rates of assimilation and oxidation implicate CH_4 as an important carbon and energy source for microbial growth in Lake Matano. By extension to other oligotrophic ferruginous environments, CH_4 was likely an important contributor to microbial metabolisms in Earth's ferruginous Precambrian oceans.

The Supplement related to this article is available online at doi:10.5194/bgd-13-1-2016-supplement.

Author contributions. A. Sturm and S. A. Crowe designed the Experimental setup and executed the experiment; they were also responsible for the data acquisition and analysis, interpretation and manuscript preparation.
D. A. Fowle was involved in inexperimental design, scientific discussion, data interpretation and manuscript preparation.
C. A. Jones conducted fieldwork and contributed to manuscript preparation.
K. Leslie helped measuring methane concentrations and reducing and interpretation methane concentration data, she also contributed to manuscript preparation.
D. E. Canfield was involved in scientific discussions, data interpretation and manuscript preparation. S. Nomosatryo and C. Henny provided logistical and field sampling support in Indonesia.

Acknowledgements. The authors thank Alfonso Mucci and Bjørn Sundby, for inspiring discussions, D. Rahim, and S. Rio are acknowledged for sampling and logistical support in Indonesia. B. Thamdrup for lending a tube furnace for CH_4 combustions. The authors are grateful to PT-INCO Tbk for in kind support. The Danish National Research Foundation provided funding for C. Jones, S. A. Crowe, and D. E. Canfield. A. Sturm and D. A. Fowle were supported by the National Science Foundation grant EAR-0 844 250.

References

Bastviken, D., Ejlertsson, J., and Tranvik, L.: Measurement of methane oxidation in lakes: a comparison of methods, Environ. Sci. Technol., 36, 3354–3361, doi:10.1021/es010311p, 2002.

Boetius, A., Ravenschlag, K., Schubert, C. J., Rickert, D., Widdel, F., Gieseke, A., Amann, R., Jorgensen, B. B., Witte, U., and Pfannkuche, O.: A marine microbial consortium apparently mediating anaerobic oxidation of methane, Nature, 407, 623–626, 2000.

Braman, R. S. and Hendrix, S. A.: Nanogram nitrite and nitrate determination in environmental and biological-materials by Vanadium(III) reduction with chemi-luminescence detection, Anal. Chem., 61, 2715–2718, doi:10.1021/ac00199a007, 1989.

Brendel, P. J. and Luther, G. W.: Development of a gold amalgam voltammetric microelectrode for the determination of dissolved Fe, Mn, O_2, and S(-Ii) in porewaters of marine and freshwater sediments, Environ. Sci. Technol., 29, 751–761, 1995.

Brown, L. R., Strawinski, R. J., and McCleskey, C. S.: The isolation and characterization of methanomonas methanooxidans Brown and Strawinski, Canadian journal of microbiology, 10, 791-799, 1964.

Buchholz, L. A., Valklump, J., Collins, M. L. P., Brantner, C. A., and Remsen, C. C.: Activity of methanotrophic bacteria in Green-Bay sediments, FEMS Microbiol. Ecol., 16, 1–8, 1995.

Caldwell, S. L., Laidler, J. R., Brewer, E. A., Eberly, J. O., Sandborgh, S. C., and Colwell, F. S.: Anaerobic oxidation of methane: mechanisms, bioenergetics, and the ecology of associated microorganisms, Environ. Sci. Technol., 42, 6791–6799, doi:10.1021/es800120b, 2008.

Canfield, D. E. and Thamdrup, B.: Towards a consistent classification scheme for geochemical environments, or, why we wish the term “suboxic” would go away, Geobiology, 7, 385–392, 2009.

Capone, D. G. and Kiene, R. P.: Comparison of microbial dynamics in marine and fresh-water sediments – contrasts in anaerobic carbon catabolism, Limnol. Oceanogr., 33, 725–749, 1988.

Cicerone, R. J. and Oremland, R. S.: Biogeochemical aspects of atmospheric methane, Global Biogeochem. Cy., 2, 299–327, doi:10.1029/GB002i004p00299, 1988.

Conrad, R.: The global methane cycle: recent advances in understanding the microbial processes involved, Environ. Microbiol., 1, 285–292, doi:10.1111/j.1758-2229.2009.00038.x, 2009.

Crowe, S. A., Jones, C., Katsev, S., Magen, C., O’Neill, A. H., Sturm, A., Canfield, D. E., Haffner, G. D., Mucci, A., Sundby, B., and Fowle, D. A.: Photoferrotrophs thrive in an Archean Ocean analogue, P. Natl. Acad. Sci. USA, 105, 15938–15943, doi:10.1073/pnas.0805313105, 2008a.

BGD
doi:10.5194/bg-2015-533

Crowe, S. A., O'Neill, A. H., Katsev, S., Hehanussa, P., Haffner, G. D., Sundby, B., Mucci, A., and Fowle, D. A.: The biogeochemistry of tropical lakes: a case study from Lake Matano, Indonesia, Limnol. Oceanogr., 53, 319–331, 2008b.

Crowe, S. A., Katsev, S., Leslie, K., Sturm, A., Magen, C., Nomosatryo, S., Pack, M. A., Kessler, J. D., Reeburgh, W. S., Roberts, J. A., Gonzalez, L., Haffner, G. D., Mucci, A., Sundby, B., and Fowle, D. A.: The methane cycle in ferruginous Lake Matano, Geobiology, 9, 61–78, 2011.

Deangelis, M. A. and Scranton, M. I.: Fate of methane in the Hudson River and estuary, Global Biogeochem. Cy., 7, 509–523, doi:10.1029/93gb01636, 1993.

Devol, A. H., Anderson, J. J., Kuivila, K., and Murray, J. W.: A model for coupled sulfate reduction and methane oxidation in the sediments of Saanich inlet, Geochim. Cosmochim. Ac., 48, 993–1004, doi:10.1016/0016-7037(84)90191-1, 1984.

Ettwig, K. F., Butler, M. K., Le Paslier, D., Pelletier, E., Mangenot, S., Kuypers, M. M. M., Schreiber, F., Dutilh, B. E., Zedelius, J., de Beer, D., Gloerich, J., Wessels, H. J. C. T., van Alen, T., Luesken, F., Wu, M. L., van de Pas-Schoonen, K. T., den Camp, H. J. M. O., Janssen-Megens, E. M., Francoijs, K. J., Stunnenberg, H., Weissenbach, J., Jetten, M. S. M., and Strous, M.: Nitrite-driven anaerobic methane oxidation by oxygenic bacteria, Nature, 464, 543-548, doi:10.1038/Nature08883, 2010.

Guerin, F. and Abril, G.: Significance of pelagic aerobic methane oxidation in the methane and carbon budget of a tropical reservoir, J. Geophys. Res.-Biogeo., 112, G03006, doi:10.1029/2006jg000393, 2007.

Hanson, R. S.: Ecology and Diversity of Methylotrophic Organisms, in: Advances in Applied Microbiology, edited by: Perlman, D., Academic Press, 3–39, 1980.

Haroon, M. F., Hu, S. H., Shi, Y., Imelfort, M., Keller, J., Hugenholtz, P., Yuan, Z. G., and Tyson, G. W.: Anaerobic oxidation of methane coupled to nitrate reduction in a novel archaeal lineage, Nature, 500, 567-570, 10.1038/nature12375, 2013.

Harrison, D. E. F.: Studies on the affinity of methanol- and methane-utilizing bacteria for their carbon substrates, J. Appl. Microbiol., 36, 301–308, doi:10.1111/j.1365-2672.1973.tb04106.x, 1973.

Harrits, S. M. and Hanson, R. S.: Stratification of aerobic methane-oxidizing organisms in Lake Mendota, Madison, Wisconsin, Limnol. Oceanogr., 25, 412–421, 1980.

BGD

doi:10.5194/bg-2015-533

Hoehler, T. M., Alperin, M. J., Albert, D. B., and Martens, C. S.: Field and laboratory studies of methane oxidation in an anoxic marine sediment – evidence for a methanogen-sulfate reducer consortium, Global Biogeochem. Cy., 8, 451–463, doi:10.1029/94gb01800, 1994.
Howard, D. L., Frea, J. I., and Pfister, R. M.: The potential for methane-carbon cycling in lake Erie, in: Proc. 14th International Association of Great Lakes Research, University of Toronto, Toronto, Ontario, 236–240, 1971.
Iversen, N. and Blackburn, T. H.: Seasonal rates of methane oxidation in anoxic marine-sediments, Appl. Environ. Microb., 41, 1295–1300, 1981.
Iversen, N., Oremland, R. S., and Klug, M. J.: Big Soda Lake (Nevada), 3. Pelagic methanogenesis and anaerobic methane oxidation, Limnol. Oceanogr., 32, 804–814, 1987.
Jannasch, H. W.: Methane oxidation in Lake Kivu (Central Africa), Limnol. Oceanogr., 20, 860–864, 1975.
Joergensen, L.: The methane mono-oxygenase reaction system studied invivo by membrane-inlet mass-spectrometry, Biochem. J., 225, 441–448, 1985.
Jones, C., Crowe, S. A., Sturm, A., Leslie, K. L., MacLean, L. C. W., Katsev, S., Henny, C., Fowle, D. A., and Canfield, D. E.: Biogeochemistry of manganese in ferruginous Lake Matano, Indonesia, Biogeosciences, 8, 2977–2991, doi:10.5194/bg-8-2977-2011, 2011.
Jørgensen, B. B., Kuenen, J. G., and Cohen, Y.: Microbial transformations of sulfur-compounds in a stratified lake (Solar Lake, Sinai), Limnol. Oceanogr., 24, 799–822, 1979.
Joye, S. B., Connell, T. L., Miller, L. G., Oremland, R. S., and Jellison, R. S.: Oxidation of ammonia and methane in an alkaline, saline lake, Limnol. Oceanogr., 44, 178–188, 1999.
Kampman, C., Hendrickx, T. L. G., Luesken, F. A., van Alen, T. A., Op den Camp, H. J. M., Jetten, M. S. M., Zeeman, G., Buisman, C. J. N., and Temmink, H.: Enrichment of denitrifying methanotrophic bacteria for application after direct low-temperature anaerobic sewage treatment, J. Hazard Mater., 227, 164–171, doi:10.1016/j.jhazmat.2012.05.032, 2012.
Kessler, J. D., Reeburgh, W. S., Southon, J., Seifert, R., Michaelis, W., and Tyler, S. C.: Basin-wide estimates of the input of methane from seeps and clathrates to the Black Sea, Earth Planet. Sc. Lett., 243, 366–375, doi:10.1016/j.epsl.2006.01.006, 2006.
Knittel, K. and Boetius, A.: Anaerobic oxidation of methane: progress with an unknown process, Annu. Rev. Microbiol., 63, 311–334, 2009.
Kroeger, K. F., di Primio, R., and Horsfield, B.: Atmospheric methane from organic carbon mobilization in sedimentary basins – the sleeping giant?, Earth-Sci. Rev., 107, 423–442, doi:10.1016/j.earscirev.2011.04.006, 2011.

BGD
doi:10.5194/bg-2015-533

Lidstrom, M. E. and Somers, L.: Seasonal study of methane oxidation in Lake Washington, Appl. Environ. Microb., 47, 1255–1260, 1984.
Liikanen, A. and Martikainen, P. J.: Effect of ammonium and oxygen on methane and nitrous oxide fluxes across sediment Äìwater interface in a eutrophic lake, Chemosphere, 52, 1287–1293, 2003.
Liikanen, A., Huttunen, J. T., Valli, K., and Martikainen, P. J.: Methane cycling in the sediment and water column of mid-boreal hyper-eutrophic Lake Kevaton, Finland, Arch. Hydrobiol., 154, 585–603, 2002.
Liikanen, A., Ratilainen, E., Saarnio, S., Alm, J., Martikainen, P. J., and Silvola, J.: Greenhouse gas dynamics in boreal, littoral sediments under raised CO_2 and nitrogen supply, Freshwater Biol., 48, 500–511, doi:10.1046/j.1365-2427.2003.01023.x, 2003.
Lilley, M. D., Baross, J. A., and Dahm, C. N.: Methane production and oxidation in lakes impacted by the 18 May 1980 Eruption of Mount St. Helens, Global Biogeochem. Cy., 2, 357–370, doi:10.1029/GB002i004p00357, 1988.
Lopes, F., Viollier, E., Thiam, A., Michard, G., Abril, G., Groleau, A., Prévot, F., Carrias, J. F., Albéric, P., and Jézéquel, D.: Biogeochemical modelling of anaerobic vs. aerobic methane oxidation in a meromictic crater lake (Lake Pavin, France), Appl. Geochem., 26, 1919–1932, doi:10.1016/j.apgeochem.2011.06.021, 2011.
Luesken, F. A., Sánchez, J., van Alen, T. A., Sanabria, J., Op den Camp, H. J. M., Jetten, M. S. M., and Kartal, B.: Simultaneous nitrite-dependent anaerobic methane and ammonium oxidation processes, Appl. Environ. Microb., 77, 6802–6807, 2011a.
Luesken, F. A., van Alen, T. A., van der Biezen, E., Frijters, C., Toonen, G., Kampman, C., Hendrickx, T. L. G., Zeeman, G., Temmink, H., Strous, M., Op den Camp, H. J. M., and Jetten, M. S. M.: Diversity and enrichment of nitrite-dependent anaerobic methane oxidizing bacteria from wastewater sludge, Appl. Microbiol. Biot., 92, 845–854, 2011b.
Luther, G. W.: Manganese(II) oxidation and Mn(IV) reduction in the environment – two one-electron transfer steps versus a single two-electron step, Geomicrobiol. J., 22, 195–203, 2005.
Martens, C. S. and Berner, R. A.: Methane production in interstitial waters of sulfate-depleted marine sediments, Science, 185, 1167–1169, 1974.
Morgan, J. J.: Kinetics of reaction between O_2 and Mn(II) species in aqueous solutions, Geochim. Cosmochim. Ac., 69, 35–48, 2005.

BGD
doi:10.5194/bg-2015-533

Nordi, K. A., Thamdrup, B., and Schubert, C. J.: Anaerobic oxidation of methane in an iron-rich Danish freshwater lake sediment, Limnol. Oceanogr., 58, 546–554, doi:10.4319/lo.2013.58.2.0546, 2013.
Raghoebarsing, A. A., Pol, A., van de Pas-Schoonen, K. T., Smolders, A. J. P., Ettwig, K. F., Rijpstra, W. I. C., Schouten, S., Damste, J. S. S., Op den Camp, H. J. M., Jetten, M. S. M., and Strous, M.: A microbial consortium couples anaerobic methane oxidation to denitrification, Nature, 440, 918–921, 2006.
Reeburgh, W. S.: Anaerobic methane oxidation – rate depth distributions in Skan Bay sediments, Earth Planet. Sc. Lett., 47, 345–352, doi:10.1016/0012-821x(80)90021-7, 1980.
Reeburgh, W. S.: Oceanic methane biogeochemistry, Chem. Rev., 107, 486–513, 2007.
Reid, R. C., Sherwood, T. K., and Prausnitz, J. M.: The Properties of Gases and Liquids, 3rd edn., McGraw-Hill, New York, 1977.
Remsen, C. C., Minnich, E. C., Stephens, R. S., Buchholz, L., and Lidstrom, M. E.: Methane oxidation in Lake-Superior sediments, J. Great Lakes Res., 15, 141–146, 1989.
Rose, S. and Long, A.: Dissolved-oxygen systematics in the Tucson Basin Aquifer, Water Resour. Res., 24, 127–136, doi:10.1029/WR024i001p00127, 1988.
Rudd, J. W. M.: Methane oxidation in Lake Tanganyika (East-Africa), Limnol. Oceanogr., 25, 958–963, 1980.
Rudd, J. W. M. and Hamilton, R. D.: Factors controlling rates of methane oxidation and distribution of methane oxidizers in a small stratified lake, Arch. Hydrobiol., 75, 522–538, 1975.
Rudd, J. W. M., Hamilton, R. D., and Campbell, N. E.: Measurement of microbial oxidation of methane in Lake Water, Limnol. Oceanogr., 19, 519–524, 1974.
Schmidt, U. and Conrad, R.: Hydrogen, carbon-monoxide, and methane dynamics in Lake Constance, Limnol. Oceanogr., 38, 1214–1226, 1993.
Shen, L.-D. and Hu, B.-l.: Microbiology, ecology and application of the nitrite-dependent anaerobic methane oxidation process, Frontiers in Microbiology, 3, 269, doi:10.3389/fmicb.2012.00269, 2012.
Sivan, O., Adler, M., Pearson, A., Gelman, F., Bar-Or, I., John, S. G., and Eckert, W.: Geochemical evidence for iron-mediated anaerobic oxidation of methane, Limnol. Oceanogr., 56, 1536–1544, doi:10.4319/lo.2011.56.4.1536, 2011.
Sloan, L. C., Walker, J. C. G., Moore, T. C., Rea, D. K., and Zachos, J. C.: Possible methane-induced polar warming in the early Eocene, Nature, 357, 320–322, doi:10.1038/357320a0, 1992.

BGD
doi:10.5194/bg-2015-533

Stookey, L. L.: Ferrozine – a new spectrophotometric reagent for iron, Anal. Chem., 42, 779–781, 1970.
Trefry, M. G. and Patterson, B. M.: An experimental determination of the effective oxygen diffusion coefficient for a high density polypropylene geomembrane, PO Wembly WA 6913, Australia, 1–21, 2001.
Treude, T., Niggemann, J., Kallmeyer, J., Wintersteller, P., Schubert, C. J., Boetius, A., and Jorgensen, B. B.: Anaerobic oxidation of methane and sulfate reduction along the Chilean continental margin, Geochim. Cosmochim. Ac., 69, 2767–2779, doi:10.1016/j.gca.2005.01.002, 2005.
Utsumi, M., Nojiri, Y., Nakamura, T., Nozawa, T., Otsuki, A., and Seki, H.: Oxidation of dissolved methane in a eutrophic, shallow lake: lake Kasumigaura, Japan, Limnol. Oceanogr., 43, 471–480, 1998a.
Utsumi, M., Nojiri, Y., Nakamura, T., Nozawa, T., Otsuki, A., Takamura, N., Watanabe, M., and Seki, H.: Dynamics of dissolved methane and methane oxidation in dimictic Lake Nojiri during winter, Limnol. Oceanogr., 43, 10–17, 1998b.
Valentine, D. L. and Reeburgh, W. S.: New perspectives on anaerobic methane oxidation, Environ. Microbiol., 2, 477–484, doi:10.1046/j.1462-2920.2000.00135.x, 2000.
Vary, P. S. and Johnson, M. J.: Cell yields of bacteria grown on methane, Appl. Microbiol., 15, 1473–1478, 1967.
Venkiteswaran, J. J. and Schiff, S. L.: Methane oxidation: isotopic enrichment factors in freshwater boreal reservoirs, Appl. Geochem., 20, 683–690, doi:10.1016/j.apgeochem.2004.11.007, 2005.
Viollier, E., Inglett, P. W., Hunter, K., Roychoudhury, A. N., and Van Cappellen, P.: The ferrozine method revisited: Fe(II)/Fe(III) determination in natural waters, Appl. Geochem., 15, 785–790, 2000.
Wankel, S. D., Joye, S. B., Samarkin, V. A., Shah, S. R., Friederich, G., Melas-Kyriazi, J., and Girguis, P. R.: New constraints on methane fluxes and rates of anaerobic methane oxidation in a Gulf of Mexico brine pool via in situ mass spectrometry, Deep-Sea Res. Pt. II, 57, 2022–2029, 2010.
Ward, B. B., Kilpatrick, K. A., Novelli, P. C., and Scranton, M. I.: Methane oxidation and methane fluxes in the ocean surface-layer and deep anoxic waters, Nature, 327, 226–229, 1987.
Whalen, S. C., Reeburgh, W. S., and Sandbeck, K. A.: Rapid methane oxidation in a landfill cover soil, Appl. Environ. Microb., 56, 3405–3411, 1990.

BGD
doi:10.5194/bg-2015-533

Wilke, C. R. and Chang, P.: Correlation of diffusion coefficients in dilute solutions, AICHE J., 1, 264–270, doi:10.1002/aic.690010222, 1955.

Zeebe, R. E., Zachos, J. C., and Dickens, G. R.: Carbon dioxide forcing alone insufficient to explain Palaeocene–Eocene Thermal Maximum warming, Nat. Geosci., 2, 576–580, doi:10.1038/ngeo578, 2009.

Zegeye, A., Bonneville, S., Benning, L. G., Sturm, A., Fowle, D. A., Jones, C., Canfield, D. E., Ruby, C., MacLean, L. C., Nomosatryo, S., Crowe, S. A., and Poulton, S. W.: Green rust formation controls nutrient availability in a ferruginous water column, Geology, 40, 599–602, doi:10.1130/g32959.1, 2012.

BGD

doi:10.5194/bg-2015-533

Table 1. Methane oxidation rates complied from a variety of global aquatic settings. Values in brackets have uncertainties with respect to oxygen concentrations during measurements.

Lake/Reservoir	Oxidation rate μmol L^{-1} d^{-1} Oxic/Oxic–Anaerobic transition/Anaerobic	Source
Lake Mendota, (Madison, Wisconsin)	28.8/4.8/5.8	Harrits and Hanson (1980)
Lake Kivu, (Africa)	0.48/0.43/0.89	Jannasch (1975)
ELA, (Nothern Ontario)	72/890	Rudd and Hamilton (1975)
Lake Pavin, (France)	0.006–0.046/–/0.4	Lopes et al. (2011)
Lake Kasumigaura, (Japan)	–/0.12/–	Utsumi et al. (1998a)
Lake Nojiri, (Japan)	–/17/–	Utsumi et al. (1998b)
Lake Erie, (USA, Canada)	–/3.84/–	Howard et al. (1971)
Big Soda Lake, (Nevada)	0.0013/0.01/0.064	Iversen et al. (1987)
Mono Lake, (California)	0.04–3.8/0.5–37/48–85 nM d-1	Joye et al. (1999)
ELARP pond, FLUDEX reservoirs (ELA)	(360–1200)	Venkiteswaran and Schiff (2005)
Petit-Saut Reservoir, (Brazil)	1600/–/–	Guerin and Abril (2007)
Lake 120 and 227, (ELA, Nothern Ontario)	1.3/–/0.49	Rudd et al. (1974)
Lake Tanganyika, (Arfrica)	0.1–0.96/0.17–1.8/0.24–1.8	Rudd (1980)
Lillsjoen lake, (Sweden)	0.33/0.01/–	Bastviken et al. (2002)
Marn lake, (Sweden)	0.81/2.17/2.2	Bastviken et al. (2002)
Illersjoen lake, (Sweden)	–/–/1.3–3	Bastviken et al. (2002)
Lake Kevätön, (Finland)	27/–/–	Liikanen et al. (2002)
Lake Matano, (Sulawesi, Indonesia)	3.6×10^{-4}–2.5×10^{-3}/0.22/4.2–117	This Study
Brine pool (Gulf of Mexico)	–/–/3.5	Wankel et al. (2010)
Cariaco Basin, (Pacific)	1×10^{-7}/1×10^{-6}/4×10^{-4}	Ward et al. (1987)
Black Sea	–/1×10^{-6}/1.64×10^{-3}	Kessler et al. (2006)
Lake Spirit, (Oregon)	0.144/0.065/–	Lilley et al. (1988)
Hudson River, (New York)	4×10^{-6}–6×10^{-4}/–/–	Deangelis and Scranton (1993)

BGD
doi:10.5194/bg-2015-533

Table 2. Availability of redox species in the incubation syringe in µmol L^{-1}, "oxidation potential (%)" is the potential contribution of each redox species towards oxidizing CH_4 to CO_2. Maximum O_2 introduction into syringes by diffusion and its possible increase of O_2 content compared to background in [%] and how much this amount of O_2 could have been part in the observed CH_4 oxidation (%). Methane oxidation to CO_2 during the incubation is displayed in nmol L^{-1} and as % of total CH_4 available, along with total CH_4 consumed.

Incubation Depth (m)	Conc. in µmol L^{-1} (%) contribution to CH_4 oxidation					Max O_2 diffusion into Syringes in µmol L^{-1}, O_2 increase wrt background conc. [%] and its CH_4 oxidation Potential (%)	CH_4 converted to CO_2/CH_4 total nmol L^{-1} (%)
	Fe_{part}	Mn_{part}	SO_4^{-2}	NO_3^- and NO_2^-	O_2		
20	0.077 (452)	0.003 (35.2)	26.52 (1.25 ×10^6)	0.4 (9.4 ×10^3)	210.5 (4.94 ×10^6)	45 [22] (1.06 ×10^6)	2.13/3.84; (0.30/0.53)
39.5	no Data	0.003 (15.8)	28.28 (5.95 ×10^5)	0.85 (9.0 ×10^3)	137.2 (1.44 ×10^6)	129 [94] (1.35 ×10^6)	4.59/5.98; (0.50/0.65)
81.7	no Data	0.003 (197.4)	24.75 (6.5 ×10^6)	4.32 (5.7 ×10^5)	58.4 (7.68 ×10^6)	13 [23] (1.79 ×10^6)	0.38/2.56; (0.02/0.13)
105	no Data	no Data	20.44 (8.7 ×10^4)	4.88 (1.0 ×10^4)	4.4 (9.4 ×10^3)	5 [114] (1.07 ×10^4)	23.5/66.2; (0.36/1.01)
110	no Data	no Data	18.93 (3.3 ×10^4)	5.39 (4.8 ×10^3)	0.25 (2.2E2)	0.022 [2.2] (19.4)	56.7/448; (2.1/16.6)
115	0.107 (2.03)	0.148 (5.62)	31.55 (4.8 ×10^3)	0.1 (7.6)	0 (0.00)	0.024 [–] (1.86)	648/1408; (7.1/15.2)
120	0.101 (20.9)	0.003 (1.24)	9.91 (1.6 ×10^4)	0.077 (64)	0 (0.00)	0.014 [–] (11.8)	60.5/732; (0.05/0.61)
130	0.097 (0.36)	0.001 (0.008)	0.25 (7.5)	0.055 (0.83)	0 (0.00)	0.014 [–] (0.216)	3330/7092; (0.63/1.47)

BGD
doi:10.5194/bg-2015-533

Table 3. Mass action equations and their corresponding Gibbs Free energy (ΔG°) of reaction at 298.15 K for demonstrated and theoretical AOM pathways.

Reaction	$\Delta G^{0'}$ in kJ mol^{-1} CH_4	Reference
$5CH_4 + 8NO_3^- + 8H^+ \rightarrow 5CO_2 + 4N_2 + 14H_2O$	−765	Raghoebarsing et al. (2006)
$3CH_4 + 8NO_2^- + 8H^+ \rightarrow 3CO_2 + 4N_2 + 10H_2O$	−928	Raghoebarsing et al. (2006)
$CH_4 + 8Fe(OH)_3 + 15H^+ \rightarrow HCO_3^- + 8Fe^{2+} + 21H_2O$	−572.2	Crowe et al. (2011)
$CH_4 + 4MnO_2 + 7H^+ \rightarrow HCO_3^- + 4Mn^{2+} + 5H_2O$	−789.9	Crowe et al. (2011)
$CH_4 + SO_4^- \rightarrow HCO_3^- + HS^- + H_2O$	−20 to −30	Boetius et al. (2000); Valentine et al. (2000)

BGD
doi:10.5194/bg-2015-533

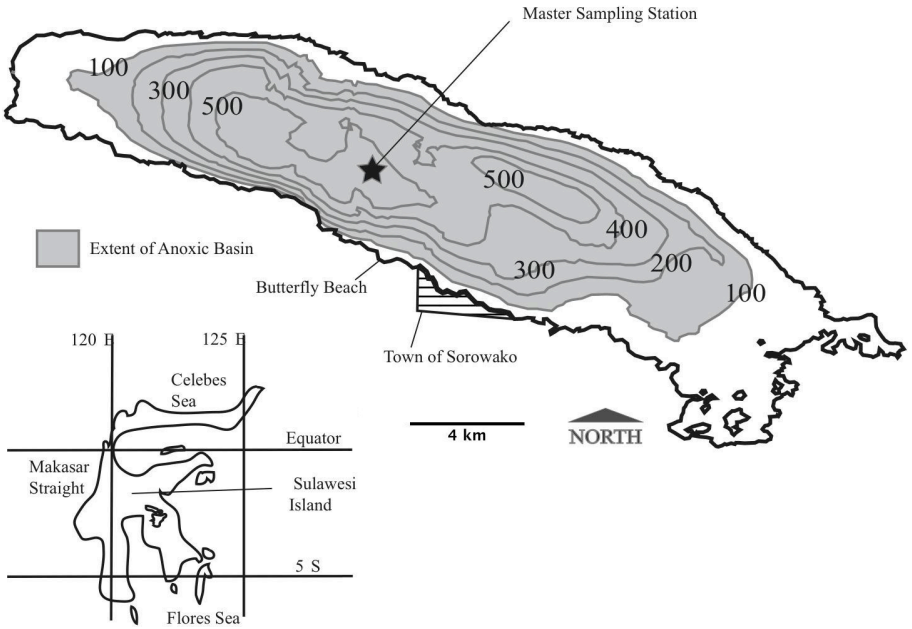

Figure 1. Map of Lake Matano bathymetry, with the extent of the anoxic basin is shaded. The location of the deep water master sampling station and the town of Sorowako are indicated (modified after Crowe et al., 2008).

BGD
doi:10.5194/bg-2015-533

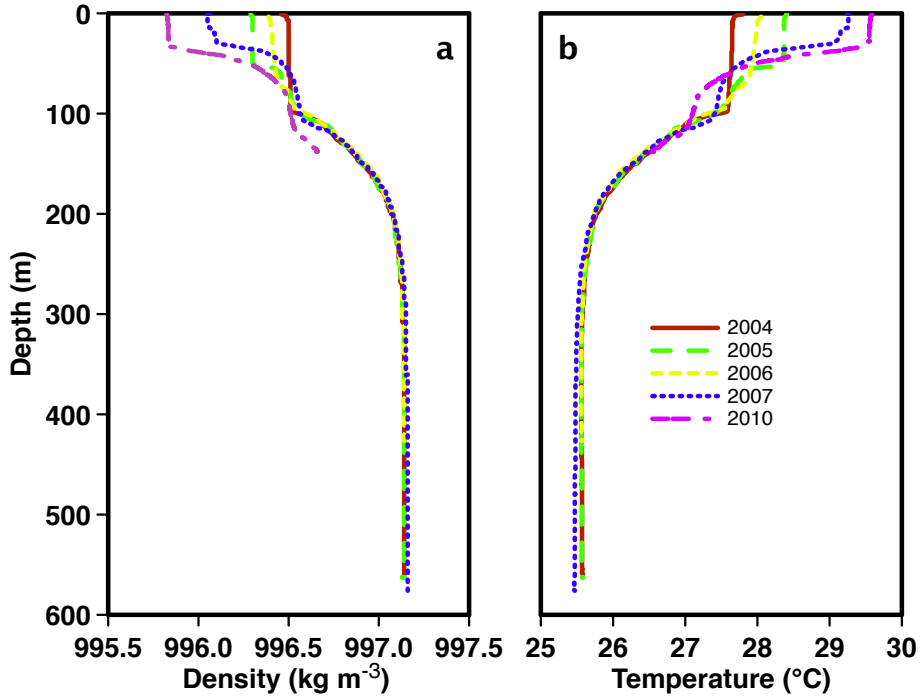

Figure 2. Multi-year density **(a)** and temperature **(b)** profiles for Lake Matano.

BGD
doi:10.5194/bg-2015-533

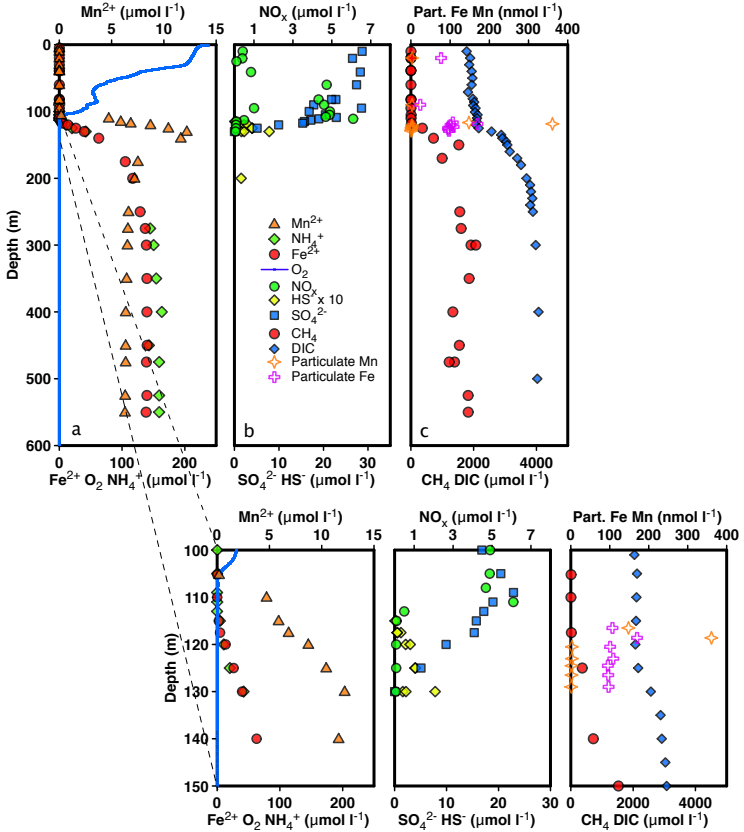

Figure 3. Lake Matano profiles for **(a)** O_2 (CTD), aqueous Fe^{2+}, Mn^{+2} and NH_4^+ **(b)** aqueous NO_x, HS^- and SO_4^{2-}, and **(c)** dissolved gases CH_4, DIC, particulate Fe and Mn (Jones et al., 2011).

BGD
doi:10.5194/bg-2015-533

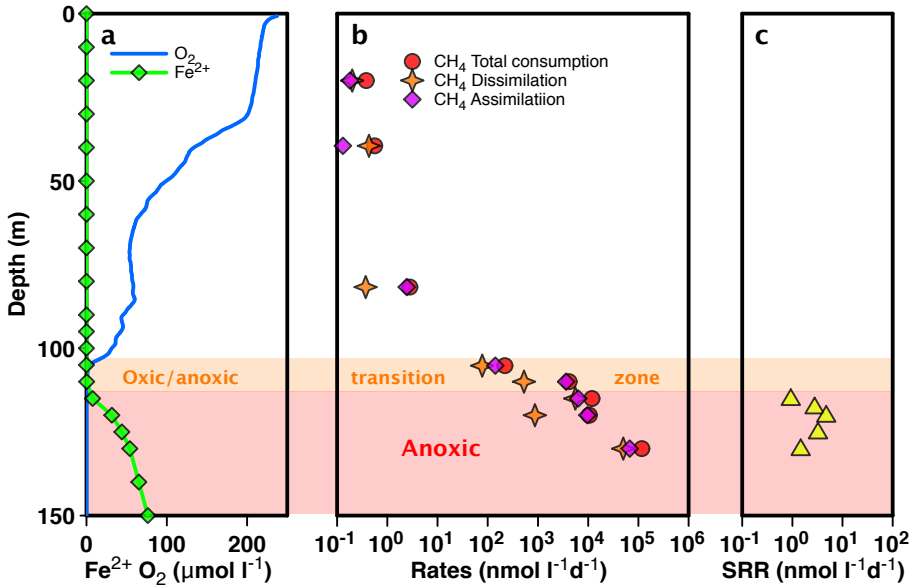

Figure 4. Dissolved biogeochemically active elements and process measurements as a function of depth **(a)** dissolved Fe^{2+} and O_2; **(b)** rates of production of CO_2 (dissimilatory CH_4 oxidation), CH_4 assimilation and total CH_4 consumption during the experiment; **(c)** sulfate reduction rates.

BGD
doi:10.5194/bg-2015-533

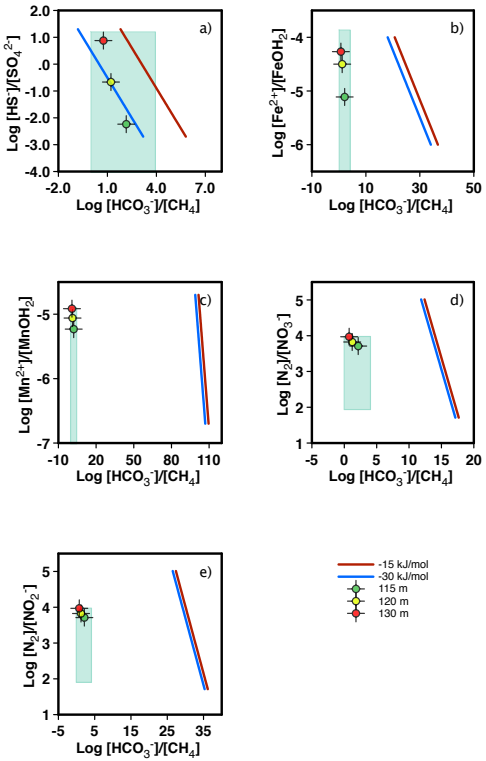

Figure 5. The plots show the energy availability at different concentrations of substrates and products for each reaction. The green areas show the range of substrate and product concentrations of Lake Matano, added are the specific anaerobic depth (115, 120, 130 m) at which our experiments were conducted. The "Iso-energy" lines show that all proposed pathways of methane oxidation are favorable except for **(a)** (SO_4^{2-}), where the $\Delta_r G$ values are very close to the previously proposed minimum values of $-15\,kJ\,mol^{-1}$ for cell survival.

BGD
doi:10.5194/bg-2015-533

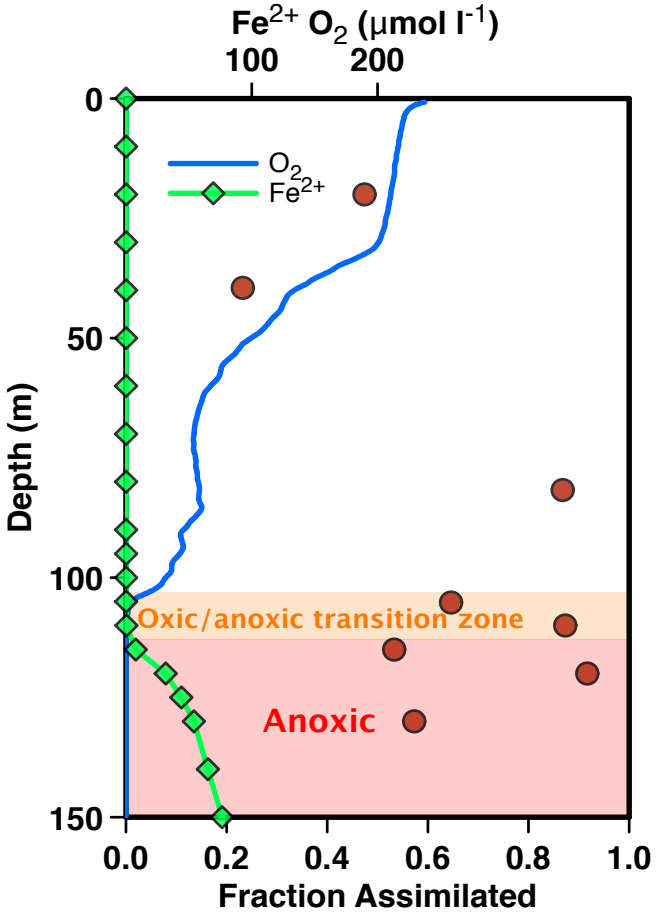

Figure 6. Fraction of CH_4 consumed through assimilation during the incubations (based on first order rate kinetics).

BGD
doi:10.5194/bg-2015-533